A novel semi-active quasi-zero stiffness vibration isolation system using a constant-force magnetic spring and an electromagnetic linear motor

Orddom Y. LEAV[1]; Carolina ERIKSSON[2]; Benjamin S. CAZZOLATO[1]; William S. ROBERTSON[1]; Boyin DING[1]

[1] School of Mechanical Engineering, University of Adelaide, Australia

[2] KTH Royal Institute of Technology, Sweden

ABSTRACT

The performance of conventional vibration isolation systems are limited by the stiffness of the mount required to support the weight of the payload. A potential method for addressing this limitation is to use the phenomenon of quasi-zero stiffness (QZS), which results in a high static stiffness to support the weight of payload and a low dynamic stiffness to achieve a wider vibration isolation range. Recently, QZS systems with various negative stiffness elements and mechanical configurations have been proposed and studied. This paper presents the design and analysis of a novel semi-active QZS vibration isolation system using a commercial constant-force magnetic spring and an electromagnetic linear motor. The proposed system combines the advantages of both passive QZS systems and active damping control, and therefore is cost-effective, energy-efficient, and has the potential of a large bandwidth of vibration isolation as well as a low resonance peak. The use of a commercial magnetic spring not only allows the system to support a large static payload over a wide range of travel but also simplifies the design. In this paper, the design, identification and control aspects of the proposed vibration isolation system are discussed and the system performance is investigated theoretically and experimentally.

Keywords: quasi-zero stiffness, semi-active control, vibration isolator
I-INCE Classification of Subjects Number(s): 46.2 and 46.3

1. INTRODUCTION

Isolating an object from a vibration source is required in a wide range of engineering applications, therefore improving the performance of vibration isolation systems is a field of ongoing research. In a conventional vibration isolation system that consists of a payload mass m supported by a linear mount stiffness k, effective vibration isolation only occurs over an excitation frequency of $\sqrt{2k/m}$ (1). This implies that a decrease in mount stiffness leads to an increase in vibration isolation frequency range or bandwidth. However, a decrease in mount stiffness can also lead to an increase in static deflection of the mass. Therefore, the performance of the conventional vibration isolation system is generally compromised by its linear mount stiffness (2).

A potential method for addressing this limitation is the use of non-linear mount stiffness in the isolator, with the aim to achieve a high static stiffness to support the weight of payload but a low dynamic stiffness to obtain a large vibration isolation bandwidth (3). This phenomenon is often referred to as quasi-zero-stiffness (QZS) and can be usually realised by combining a negative stiffness element with a positive stiffness element in the isolator. In the last decade, various QZS vibration isolation systems with various negative stiffness elements (e.g. magnets, oblique springs and Euler buckled beams) and mechanical configurations were proposed and studied (1, 4, 5, 6, 7, 8,

[1] Orddom.leav@student.adelaide.edu.au
[2] Carerikss@kth.se

9, 10).

In general, a QZS vibration isolation system is designed as fully passive system such as those demonstrated in (1, 4, 5, 7, 8, 9, 10) but can be easily extended to a semi-active system by adding an actuator and adjusting the system properties in real-time (6, 11, 12). Passive QZS isolators are not robust under varying conditions such as excitation changes or system parameter changes, since their force-displacement characteristics are tuned according to the operating conditions (6, 13). On the other hand, fully active isolators are much more robust in performance but are not cost-effective (14). Semi-active isolators combine the merits from both technologies and therefore have the advantage of passive isolators in terms of supporting the weight of payload to reduce total power consumption and also have the advantage of an active isolator in terms of achieving optimal performance in an adaptive manner (6, 14).

In this work, a novel semi-active QZS vibration isolation system is proposed and investigated, which consists of a commercial constant-force magnetic spring acting as a passive QZS isolator and an electromagnetic linear motor for achieving active damping control. The commercial constant-force magnetic spring is used due to its constant static loading capacity over a wide range of travel and also its compactness. The characteristic of constant-force magnetic springs differ from the characteristics of nonlinear elements studied so far for achieving QZS and hence is valuable to the field of research. The electromagnetic linear motor is selected due to its compactness, fast response, ease of maintenance and ease of integration with a standard control system [6]. The proposed semi-active QZS isolator combines the advantages of both passive QZS systems and active damping control, and therefore is cost-effective, energy-efficient, and has a large bandwidth of vibration isolation, as well as a low resonance peak. Although demonstrated as a single-axis vibration isolator in this paper, the idea can be simply extended to three-dimensional vibration isolation by arranging six proposed semi-active QZS isolators in a Stewart platform configuration, thereby isolating all six DOFs.

The aim of this paper is to present the design and analysis of the proposed semi-active QZS vibration isolation system. In Section 2, the design of the isolator is described followed by the characteristics, modelling and control of the isolation system. Section 3 demonstrates the numerical simulation results on both the fully passive QZS isolator without active damping control and the semi-active QZS isolation system with active damping control. The experimental studies on both the fully passive isolator and the semi-active isolation system are covered in Section 4. Section 5 concludes the study and leads to future work.

2. THE SEMI-ACTIVE QZS VIBRATION ISOLATION SYSTEM

As shown in Figure 1, the proposed semi-active QZS vibration isolation system consists of a nonlinear magnetic spring, termed as MagSpring (M01-37x230/200, LinMot) and an electromagnetic linear motor (PS01-23X80 with PL01-12X290/240 stator, LinMot) mounted in parallel to a linear guide (H01-23x86, LinMot). The MagSpring has built-in permanent magnets generating a nominal constant force of ±60N over its travel range of 200mm and behaves as a QZS isolator for static payload support and passive vibration isolation. The linear motor is used to enable additional active control on the mechanism and has a maximum force capacity of 44N and a stroke length of 240mm. The linear guide functions as a block that couples the MagSpring and the linear motor and has two linear rails with extremely low-friction bearings, which constrains the movement of the isolation system along its longitudinal axis. The linear guide has hard stops on both ends, which reduces the permissible stroke of the isolation system to 160mm.

The following subsections present the characteristics of the MagSpring, theoretical modelling and identification of the isolation system, and control aspects of the system.

2.1 Characteristic of the System

The literature shows that there exist numerous methods that utilise non-linear elements with positive and negative stiffness to realise a QZS mechanism. Two typical QZS mechanisms with unique force/displacement characteristics are oblique spring elements and magnet elements. The combination of two oblique springs and a vertical spring produce a cubic force/displacement characteristic, whereas using three vertical magnets Robertson et al. (15) obtained a quadratic force/displacement characteristic. Although exhibiting different force/displacement characteristics, these QZS mechanisms had a common goal; to achieve almost zero stiffness at the equilibrium position for better vibration isolation, but also a large stiffness away from the equilibrium position

Figure 1 – Photo of the semi-active QZS vibration isolation system

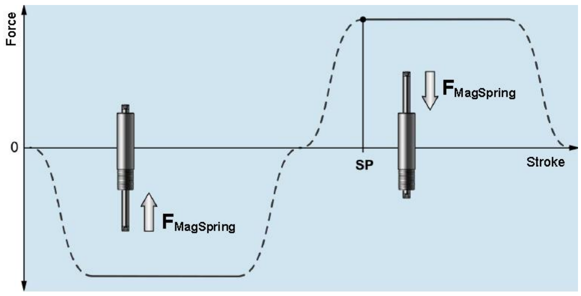

Figure 2 – Force/displacement characteristics of three QZS mechanisms (16)

for maintaining the stability of the system. Therefore, these QZS mechanisms normally had a trade-off between their static loading capacity at the equilibrium position and their vibration isolation performance.

The nominal force/displacement characteristic of the commercial MagSpring used in this project was provided by the manufacturer and is shown in Figure 2. The MagSpring can operate under both compression and tension. Under compression, the MagSpring generates a constant force of 60N within its constant-force region, which has a range of approximately 60mm. The MagSpring has the same behaviour under tension but with a constant force of -60N. Within the constant-force region, the stiffness of the MagSpring is nominally zero, which results in a large bandwidth of vibration isolation. In addition, the constant force generated by the MagSpring can be used to support a static payload. However, since the stiffness is zero within the constant-force region, the system is marginally stable and additional active control is required to maintain the MagSpring within its constant-force region. In the proposed design, the MagSpring will be operational under compression only caused by the weight of the payload. The characteristics of the MagSpring differ from the characteristics of nonlinear elements studied so far for achieving QZS and hence have potential research value. In this paper, the MagSpring is treated as a black box whose behaviour is identified and modelled for both theoretical and experimental studies on the integrated vibration isolation system.

2.1.1 Theoretical Model

The vibration isolation system was modelled mathematically to enable a theoretical investigation and numerical simulation to be conducted. To aid in the modelling, a number of assumptions were made as listed below:

1) The isolation system can only move along its longitudinal axis. The other five axes in three-dimensional space are assumed to be completely rigid.
2) All the movable parts including motor shaft, MagSpring shaft, linear guide shafts, and the payload are assumed to be a lumped mass.
3) Sensor dynamics and motor dynamics are assumed to be negligible in this paper.
4) Fixation between the isolation system and the shaker is completely rigid so that shaker force is directly transmitted to the isolation system.
5) The motion of the isolation system is limited within the stroke range of the linear guide.

With the above assumptions, the isolation system can be simplified as a mass-spring-damper-actuator system shown in Figure 3. Analysis of the force balance on the top movable mass results in the following differential equation:

$$m\ddot{x} = F_{\text{spring}}(y - x) + F_{\text{friction}}(\dot{y} - \dot{x}) + F_{\text{control}} - mg \quad (1)$$

where m represents the top movable mass, x represents the absolute position of the moveable mass, y represents the absolute position of the vibration ground/shaker end-effector, F_{spring} represents the force generated by the MagSpring, which is a function of the position of the movable mass with respect to the vibration ground, F_{friction} represents the total friction force within the system which is a function of the velocity of the movable mass with respect to the vibration ground, F_{control} represents the control force generated by the linear motor, and g represents the gravitational acceleration. Based on the force/displacement characteristic shown in Figure 2, F_{spring} can be reasonably estimated using a hyperbolic tangent function within the stroke of MagSpring and therefore,

$$F_{\text{spring}}(y-x) = a \cdot \tanh[b(y-x)] \tag{2}$$

where a and b determine the amplitude and transient interval of the hyperbolic tangent function respectively. The total friction force within the system results from the friction force in the MagSpring as well as the friction force in the motor and can be decoupled to stiction, Coulomb friction and viscous friction (17):

$$F_{\text{friction}}(\dot{y}-\dot{x}) = -\left[F_{\text{c}} + (F_{\text{s}} - F_{\text{c}})e^{-C_{bc}|\dot{y}-\dot{x}|}\right] \cdot \text{sign}(\dot{y}-\dot{x}) - C_{\text{v}}(\dot{y}-\dot{x}), \tag{3}$$

where F_{c} represents the Coulomb friction, F_{s} represents the stiction force, C_{bc} represents a coefficient that determines the transition speed from stiction to Coulomb friction and C_{v} represents the viscous friction coefficient. When the force acting on the payload is not high enough to conquer the stiction, the motion of the payload relative to the shaker will be 'locked'. This 'locked' motion due to stiction causes the relative motion between the payload and shaker to be zero ($\dot{x} = \dot{y}$). When the force acting on the payload overcomes the stiction, the motion of the system will be 'unlocked' and the total friction force acting on the payload will be described by Equation (3). The vibration isolator will return to its 'locked' state if the force is less than stiction.

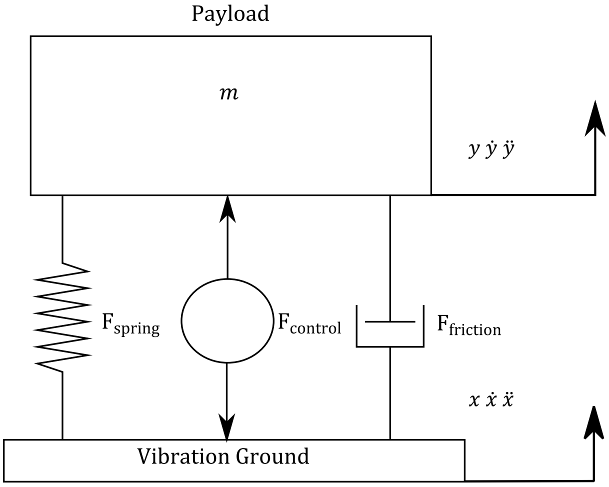

Figure 3 – Simplified model of the isolation system

2.1.2 System identification

A material testing machine (8500, Instron, Inc.) was used to identify the parameters of the model described in Equation (3). The testing set-up is shown in Figure 4. The MagSpring was fixed vertically via an angle plate to the ground and was coupled to the hydraulic actuator of the testing machine via a load-cell (ALD-.75MINI-UTC-M, A.L. Design, Inc) and a custom made X-Y table. The load-cell was used to measure the reaction force on the MagSpring and the X-Y table was used to minimize the shear forces on the testing rig caused by any misalignment in set-up in order to protect the load-cell and isolation system from damage. Under the regulation of hydraulic actuator, the position of the MagSpring was controlled at a number of static positions over its stroke range while the corresponding load-cell measurements at these positions were recorded. The static force/displacement relationship from measurements is shown in Figure 5, as well as the fitted hyperbolic tangent curve from Equation (2) with $a = -60.84$ and $b = 78.10$ that approximates the measured characteristic.

To identify the parameters of the friction model, the MagSpring, linear motor and the fully integrated isolation system were also tested by the material testing machine under dynamic waveform positioning. The identification process was tedious and hence is not discussed in this paper in detail. Essentially the viscous friction coefficient was estimated from the energy dissipation of the system. Stiction and Coulomb friction were estimated by observation of the instantaneous change in the measured force. Table 1 shows the parameters of the model identified from experiments, as well as some commonly used parameters. In Section 3.1, numerical simulations are used to validate and optimise some of these measured parameters to better model the system behaviour, which is in fact fully nonlinear.

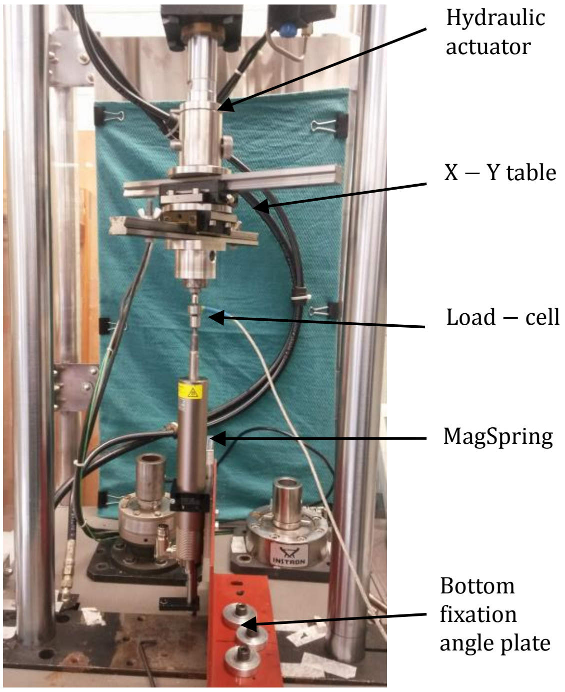

Figure 4 – The MagSpring undergoing testing using an Instron material testing machine

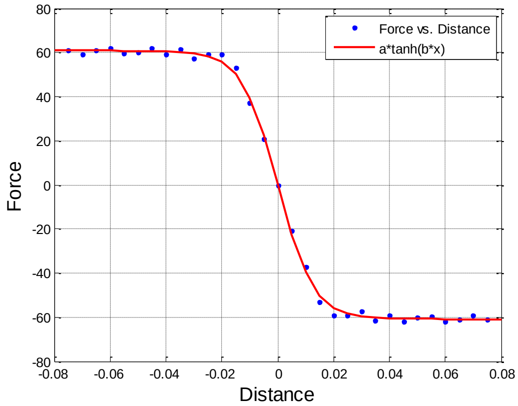

Figure 5 – Static force-displacement characteristic of the MagSpring where the fitted curve is defined by $a = -60.84$ N and $b = 78.10$ m^{-1}

Table 1 – Parameters of the system model

Parameter	Physical meaning	Value
m	Mass of the total top movable mass	6.4kg
g	Gravity acceleration	9.81m/s^2
a	Amplitude of MagSpring constant force	60.84N
b	Coefficient determining MagSpring transient interval	78.10m^{-1}
F_s	Stiction Force	10N
F_c	Coulomb friction	1N
C_{bc}	Coefficient determines static friction transition speed	100Ns/m
C_v	Viscous friction coefficient	100Ns/m

2.2 Control of the System

Since the MagSpring is marginally stable (as described in Section 2.1), additional control effect is required to stabilize the passive system. Furthermore, active damping control can be used to further enhance the performance of the semi-active isolation system. Figure 6 shows the control algorithm applied to the semi-active isolator. A low bandwidth/slow PI controller is used to maintain the position of the MagSpring within the middle of its stroke. This not only prevents the linear guide from over-travel but also keeps the MagSpring working near an operating point, without suffering from any underlying non-linearity over its stroke length. The PI control loop is closed by the motor position encoder feedback. Therefore, there is a risk that the controller can physically increase the stiffness of the closed loop system, which can degrade low frequency vibration isolation performance. Intuitively the higher the PI gains, the worse the vibration isolation at low frequency but the better the position tracking on the MagSpring and versa vice. This is assessed using various PI gains and is presented in the results section. In parallel with the low bandwidth PI controller, a high bandwidth/fast damping control is used to further suppress the resonances within the system based on the velocity feedback of the top payload. The velocity feedback can be obtained by integrating the acceleration measured by an accelerometer mounted on the top payload, then multiplying the velocity feedback by a proportional gain results in the damping control signal. The combination of the integration process and proportional gain is equivalent to an integral gain controller with acceleration input. The total motor control signal is then given by the superposition of the control signal from the low bandwidth PI controller and the control signal from the high bandwidth damping controller. The performance of damping control with various control gain is also assessed in the results section.

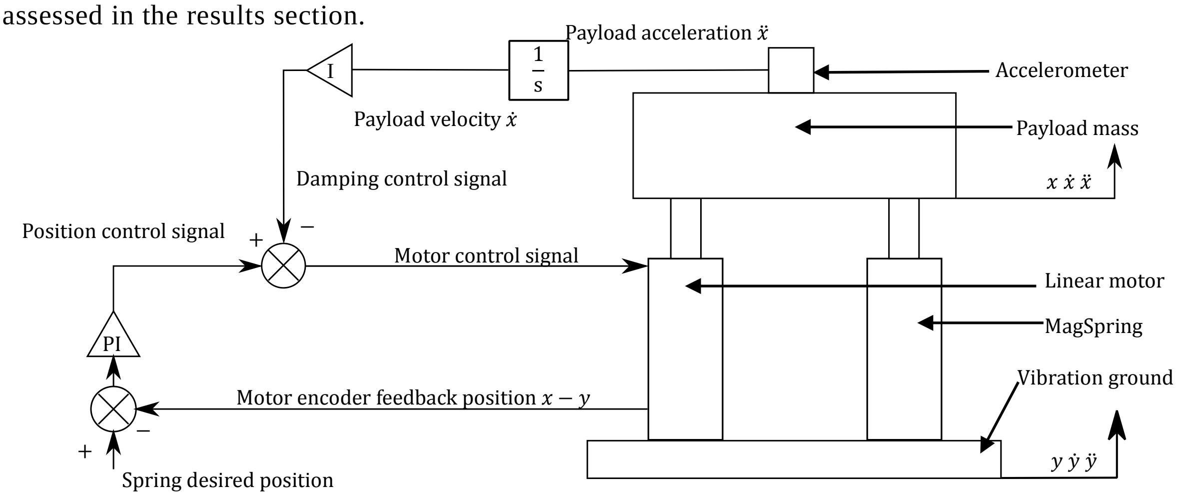

Figure 6 – Control algorithm for the semi-active isolator: magnetic spring position control + active damping control

3. NUMERICAL SIMULATIONS AND ANALYSIS

The mathematical model of the QZS isolation system can be solved numerically using Simulink to gain an understanding of the performance of the isolator. The Simulink model used to numerically simulate the behaviour employed a constant position amplitude (10mm) chirp signal from 0Hz to 20Hz. The Simulink model contains the mathematical model described in Section 2.1.1. The encoder position controller and the payload velocity controller are also comprised in the model. The numerical solver used in Simulink is a fixed-step numerical ordinary differential equation solver (ODE-3). The numerical simulations results are expressed in a transmissibility analysis of the power spectral density ratio of the shaker acceleration and payload/ isolating mass acceleration. The power spectral density in the numerical simulations uses a Hanning window with a FFT length of 32768 and 122 averages.

3.1 Passive QZS Isolator

To quantify the non-linear behaviour of the passive QZS isolator, the parameters in the friction model were varied around their initial values obtained from measurements. In the real system, stiction can vary a little throughout the stroke of the system and therefore was investigated in the numerical simulation around its initial value (10N) obtained from measurements. The remaining friction parameters were held constant with the values in Table 1. Figure 7 shows the transmissibility of the isolator with varying stiction thresholds. Stiction increases the transmissibility of the isolator at low frequencies due to the ‘locked’ motion. With the increase of the stiction, the bandwidth of vibration isolation is decreases. Furthermore, since the stiffness of the system is in theory zero and the mass is of the system is significant, the resonance of the system is very low at approximately 0.08Hz. Hence, stiction masks the effects of resonance in the system, which is desirable for vibration isolation performance.

The viscous friction of the system is in fact also nonlinear and can change throughout the stroke of the system, as well as at different velocities. Therefore, the viscous coefficient of friction in the numerical simulation was varied, with the remaining friction parameters held constant at the values in Table 1. It can be seen from the simulation results in Figure 8 that at frequency range higher than 3Hz, the system’s isolation performance is governed by the viscous friction. By increasing the viscous friction it results in a higher transmissibility at higher frequencies and a slower roll-off for vibration isolation. This is due to the fact that system with higher viscous damping is more likely to be ‘locked’ by the stiction as the relative velocity will decrease with the increase of friction force.

Consequently, the system switches between "locked' and 'unlocked' states frequently, which can degrade its isolation performance.

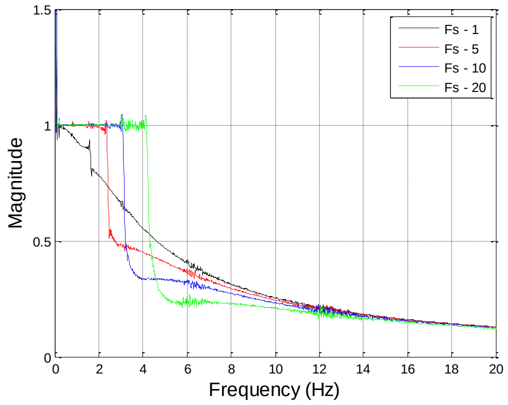

Figure 7 – Transmissibility for numerical simulation with varying stiction force over the range of 0-20Hz

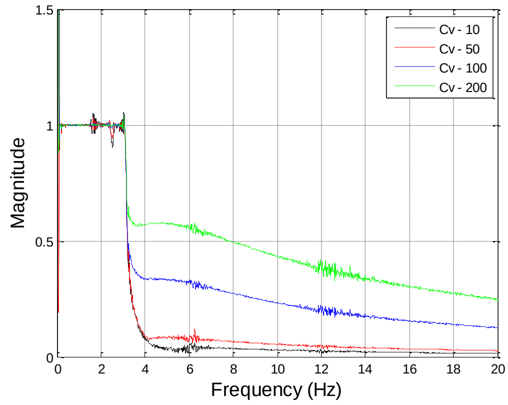

Figure 8 – Transmissibility for numerical simulation with varying viscous friction coefficient over the range of 0-20Hz

The motor encoder position control loop has been applied to the passive system with parameters shown in Table 1 and the effects of varying control gains have been investigated. Four sets of PI control gains in the encoder feedback have been chosen and Figures 9 (0-20Hz) and 10 (0-5Hz) show the transmissibility of the system controlled by these four sets of PI gains. It can been seen that at the higher frequency range performance does not change substantially with varying PI gains, but the low frequency performance is affected. The results in Figure 9 show that the system's performance for vibration isolation at lower frequencies is barely affected by low PI gains, but significantly deteriorates with excessively high PI gains. The addition of the proportional gain will also change the resonance in the system to a range of values between 0.08Hz-0.45Hz, but due to stiction the effects of resonance remain masked. Hence, PI gains need to be set as low as possible so long as the gains can maintain the position of the isolator near its operating point.

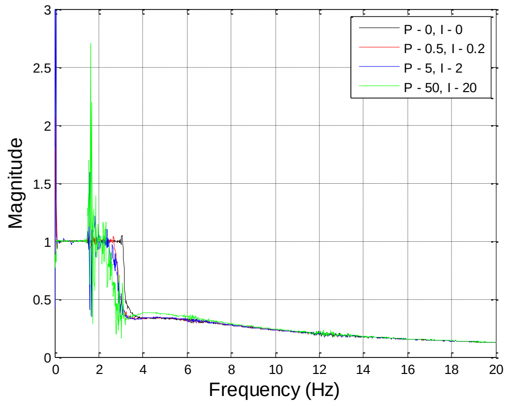

Figure 9 – Transmissibility for numerical simulation with passive PI control QZS vibration isolation over the range of 0-20Hz

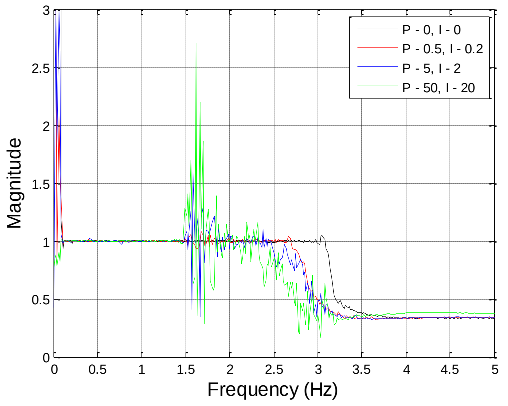

Figure 10 – Transmissibility for numerical simulation with passive PI control QZS vibration isolation over the range of 0-5Hz

4. Experimental Studies

The experimental set-up is shown in Figure 11 where the semi-active vibration isolation system was mounted on a dynamic shaker (V271, LDS, Inc.) via a rigid MayTec extrusion for testing its vibration isolation performance. A 5.5kg payload was added on the top to offset the static force of the MagSpring and to minimize the control efforts from the linear motor. A counterweight was used to balance the moments resulting from the weight of the isolation system. One accelerometer (4384, Bruel & Kjaer, Inc) was magnetically mounted on the top of the payload and was used for both damping control and payload acceleration recording. Another accelerometer was magnetically mounted on the counter weight to record the acceleration of vibration source. This project used a dSpace controller (DS1104) as the primary controller, which implements the motor control algorithm described in Figure 6, generates the shaker control signal in an open loop manner, and logs the velocity data output by two charge amplifiers (2635, B&K, Inc.) for analysis. A motor amplifier (E1200-GP-UC, LinMot, Inc.) drives the linear motor based on the motor control signal from dSpace in a current controlled mode. A shaker amplifier (PA1000L, LDS, Inc.) drives the shaker based on the shaker control signal from dSpace.

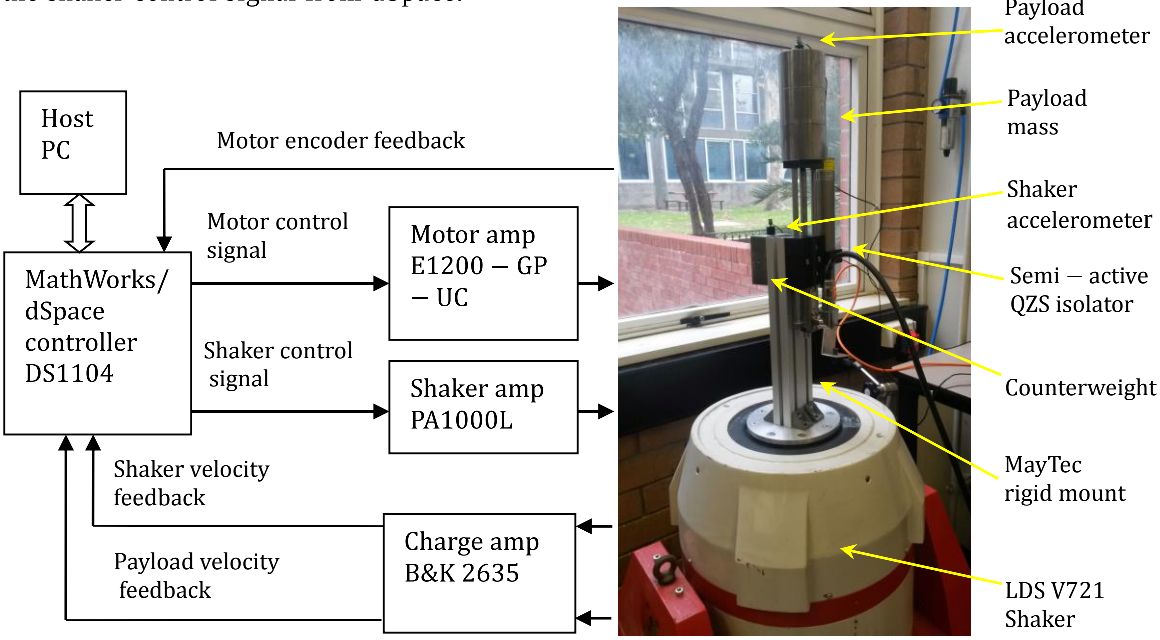

Figure 11 – Experimental set-up

4.1 Passive QZS Isolator

To validate the real performance of the passive QZS isolator, experimental testing was conducted with the system shown in Figure 11. Testing was completed with four sets of PI gains in the controller to observe the passive performance of the system with PI control. The system was excited by the shaker using a constant amplitude chirp signal. The chirp signal was generated by the dSpace controller with a sweep frequency from 0-20Hz. The velocity responses of both the shaker and isolating/top movable mass were output by the charge amplifiers that integrate the acceleration signal measurements from the two accelerometers. On the charge amplifier, a high pass filter (1Hz) was used to filter out the low frequency 'drifting' in the velocity response, which can degrade the performance of damping control. Therefore frequencies below 1Hz were not accurately measured. The experimental results for transmissibility of the passive system are shown in Figures 12 (0-20 Hz) and 13 (0-5 Hz). The experimental transmissibility results were calculated using the same method as in Section 3. The transmissibility analysis uses a Hanning window with a FFT length of 32768 and 29 averages in the data for power spectral density calculations.

The information at frequencies below 1.5Hz are not accurately represented due to the effect of the high pass filter. From the results it is evident that the transmissibility of the system is high at low frequencies as stiction is dominant in the system's behaviour. At higher frequencies the passive QZS isolator overcomes stiction and the effects of stiction in the performance of the QZS isolator become minimal. In addition, in the absence of the PI controller the MagSpring did not remain within the constant-force region and the payload mass impacted on the hard stop limits of the linear guide, which degraded its isolation performance. It can be seen from Figure 12 that in the absence of the PI controller the transmissibility is higher at higher frequencies as indicated by the black line. This issue was solved with the PI controller maintaining a position in the middle stroke of the QZS isolator. From the gain settings chosen it can be seen in Figure 12 that the PI position control improved the isolation performance at middle frequencies However, from Figure 13 it is evident that the transmissibility at lower frequencies increased with the increase of the PI control gains as PI control implicitly increased the stiffness of the system. Therefore, care must be taken when selecting the PI control gains which need to be just high enough to stabilise the MagSpring.

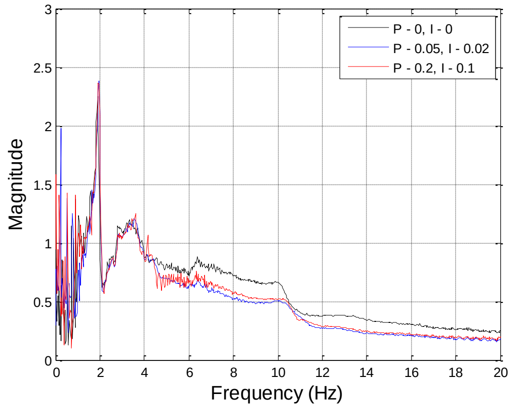

Figure 12 – Transmissibility for experimental testing with passive QZS vibration isolation over the range of 0-20Hz for three different gains

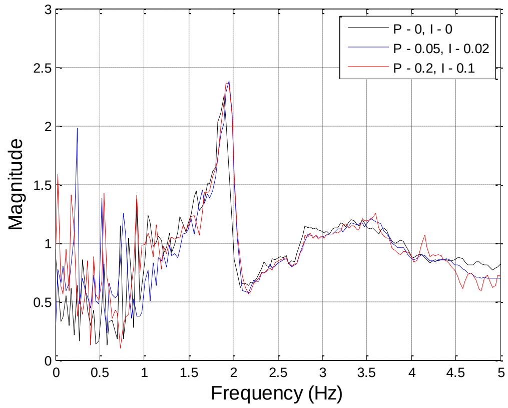

Figure 13 – Transmissibility for experimental testing with passive QZS vibration isolation over the range of 0-5Hz for three different gains

4.2 Semi-active QZS Isolation System with Active Damping Control

The performance of the semi-active vibration isolation system with active damping control was also investigated experimentally. The system was excited with the same chirp signal as described in Section 4.1 to maintain consistency in the experimental results. The testing was done with a PI gain setting of 0.05 and 0.02, respectively and three different damping gains in the system. The transmissibility results from the experimental testing can be seen in Figures 14 (0-20 Hz) and15 (0-5 Hz).

From Figures 14 and 15 it is observed that the addition of damping control did not significantly improve the performance of the system. This could be a result of the relatively high viscous friction already existing in the system. Due to the presence of significant peaks in the experimental results, active damping is to be further investigated in an attempt to attenuate the peaks.

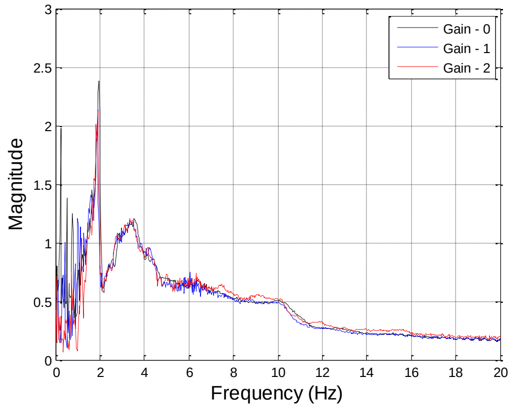

Figure 14 – Transmissibility for experimental testing with semi-active QZS vibration isolation over the range of 0-20Hz

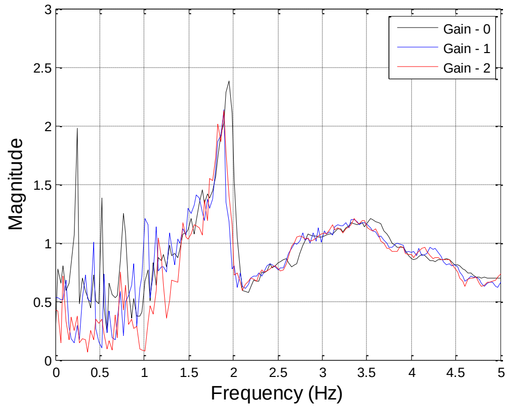

Figure 15 – Transmissibility for experimental testing with semi-active QZS vibration isolation over the range of 0-5Hz

5. CONCLUSIONS

A novel single degree of freedom semi-active QZS vibration has been designed and preliminary investigation has been undertaken numerically and experimentally to quantify the behaviour of the system. Numerical simulations demonstrated that stiction with excessive viscous friction can decrease the isolation bandwidth of the system. Both numerical simulation and experimental testing showed that with appropriate PI control, the passive system can be successfully stabilized.

Experimental results also demonstrated that the vibration isolation performance of the passive system was satisfied with resonance peaks occurring at frequencies below 3.5 Hz. The transmissibility started to roll off quickly at 4Hz and reached 0.3 at 12Hz. The addition of damping control in the system however did not improve the system performance, which requires further investigation. Future work will focus on studying the design and characteristic of the MagSpring and attempting to remove stiction in the system to achieve better isolation performance. Future work will also attempt to develop a six degree of freedom isolator based on the concept of the proposed semi-active vibration isolation system and a Stewart platform manipulator.

ACKNOWLEDGEMENTS

The authors would like to sincerely thank Mr Richard Stanley and Mr Peter Hardy for their kind assistance in system identification. The authors would also like to thank the staff in the Mechanical and Electrical Workshop of the School of Mechanical Engineering, the University of Adelaide for their assistance in mechanical design and electrical system development.

REFERENCES

1. Carrella, A, Brennam, MJ, Waters, TP. Static anlysis of a passive vibration isolator with quasi-zero-stiffness characteristic. *Journal of Sound and Vibration*. 2007; 301: 678-689.
2. Den Hartog, JP. Mechanical Vibrations. New York, USA: McGraw-Hill; 1956.
3. Alabuzhev, P, Gritchin, A, Kim, L, Migirenko, G, Chon, V, Stepanov, P. Vibration Protecting and Measuring Systems with Quasi-Zero Stiffness. New York, USA: Heishpere; 1989.
4. Carrella, A, Brennan, MJ, Waters, TP, Shin, K. On the design of a high-static-low-dynamic stiffness isolator using linear mechanical springs and magnets. *Journal of Sound and Vibration*. 2008; 315: 712-720.
5. Robertson, WS, Kidner, MRF, Cazzolato, BS, Zander, AC. Theoretical design parameters for a quasi-zero stiffness magnetic spring for vibration isolation. *Journal of Sound and Vibration*. 2009; 326: 88-103.
6. Zhou, N, Liu, K. A tunable high-static-low-dynamics stiffness vibration isolator. *Journal of Sound and Vibration*. 2010; 329: 1254-1273.
7. Xu, D, Yu, Q, Zhou, J, Bishop, SR. Theoretical and experimental analyses of a nonlinear magnetic vibration isolator with quasi-zero-stiffness characteristic. *Journal of Sound and Vibration*. 2013; 332: 3377-3389.
8. Liu, X, Huang, X, Hua, H. On the characteristics of a quasi-zero stiffness isolator using Euler buckled beam as negative stiffness corrector. *Journal of Sound and Vibration*. 2013; 332: 3359-3376.
9. Robertson, WS, Cazzolato, BS, Zander, AC. Horizontal stability of a quasi-zero stiffness mechanism using inclined linear springs. *Acoustics Australia*. 2014; 42(1): 8-13.
10. Wu, W, Chen, X, Shan, Y. Analysis and experiment of a vibration isolator using a novel magnetic spring with negative stiffness. *Journal of Sound and Vibration*. 2014; 333(13): 2958-2970.
11. Tao. Z, Cazzolato BS, Robertson, WS, Zander, AC. The development of a 6 degree of freedom quasi-zero stiffness maglev vibration isolator with adaptive-passive load support. Proceedings of 15th International Conference on Mechatronics Technology; 30 November - 2 December 2011; Melbourne, Australia 2011.
12. Robertson, WS, Cazzolato, BS, Zander, AC. Experimental results of a 1D passive magnetic spring approaching quasi-zero stiffness and using active skyhook damping. Proceedings of Acoustics 2013; 17-20 November 2013; Adelaide, Australia 2013.p. 1-8.
13. Robertson, WS, Cazzolato, BS, Zander, AC. Theoretical analysis of a non-contact spring with inclined permanent magnets for load-independent resonance frequency. *Journal of Sound and Vibration*. 2012; 331(6): 1331-1341.
14. Liu, Y, Waters, TP, Brenan MJ. A comparison of semi-active damping control strategies for vibration isolation of harmonic disturbances. *Journal of Sound and Vibration*. 2005; 280: 21-39.
15. Robertson, W, Wood, R, Cazzolato, B, Zander, A. Zero-stiffness magnetic springs for active vibration isolation. Proceedings of 6th International Symposium on Active Noise and Vibration Control; 18-20 September 2006; Adelaide, Australia 2006.
16. LinMot, Inc. MagSpring – Magnetic Springs. Elkhorn, USA; 2013.
17. MathWorks, Inc. Translational Friction. [cited 12 July 2014]. Available from: http://www.mathworks.com.au/help/physmod/simscape/ref/translationalfriction.html